

Original citation:

Miller, Thomas S., Ebejer, Neil, Guell, Aleix G., Macpherson, Julie V. and Unwin, Patrick R.. (2012) Electrochemistry at carbon nanotube forests: sidewalls and closed ends allow fast electron transfer. Chemical Communications, Volume 48 (Number 60). pp. 7435-7437. ISSN 1359-7345

Permanent WRAP url:

<http://wrap.warwick.ac.uk/54254/>

Copyright and reuse:

The Warwick Research Archive Portal (WRAP) makes the work of researchers of the University of Warwick available open access under the following conditions. Copyright © and all moral rights to the version of the paper presented here belong to the individual author(s) and/or other copyright owners. To the extent reasonable and practicable the material made available in WRAP has been checked for eligibility before being made available.

Copies of full items can be used for personal research or study, educational, or not-for-profit purposes without prior permission or charge. Provided that the authors, title and full bibliographic details are credited, a hyperlink and/or URL is given for the original metadata page and the content is not changed in any way.

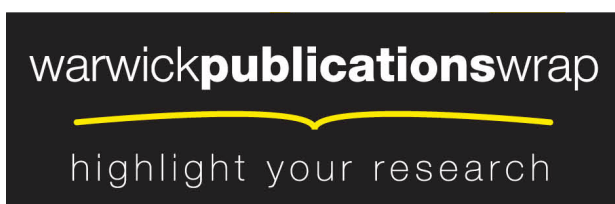
Publisher's statement:

None

A note on versions:

The version presented here may differ from the published version or, version of record, if you wish to cite this item you are advised to consult the publisher's version. Please see the 'permanent WRAP url' above for details on accessing the published version and note that access may require a subscription.

For more information, please contact the WRAP Team at: wrap@warwick.ac.uk



<http://go.warwick.ac.uk/lib-publications>

Cite this: DOI: 10.1039/c0xx00000x

www.rsc.org/xxxxxx

ARTICLE TYPE

Electrochemistry at Carbon Nanotube Forests: Sidewalls and Closed Ends Allow Fast Electron Transfer

Thomas S. Miller^{al}, Neil Ebejer^{al}, Aleix G. Güell^a, Julie V. Macpherson^{*a} and Patrick R. Unwin^{*a}*Received (in XXX, XXX) XthXXXXXXXXX 20XX, Accepted Xth XXXXXXXXXXXX 20XX*

DOI: 10.1039/b000000x

The electrochemical properties of the closed ends and sidewalls of pristine carbon nanotube forests are investigated directly using a nanopipet electrochemical cell. Both are shown to promote fast electron transfer, without any activation or processing of the carbon nanotube material required, in contrast to the current model in the literature.

Carbon nanotubes (CNTs) are of considerable interest for a wide variety of applications and can be arranged in a multitude of different geometries, ranging from 1D isolated tubes to 2D planar arrays and random networks, and 3D forests. The forest is particularly interesting with wide ranging applications.^{1,2,3} In the electrochemical arena, forests have been proposed for sensing and energy applications,⁴ with the vast majority of studies focusing on forests with open ends. Open ends also provide sites for surface functionalisation.⁵ Open-ended CNT forests have also been proposed as the preferred arrangement for electrochemistry,⁶ since some work has suggested that heterogeneous electron transfer occurs much more readily at open ends than sidewalls, with sidewalls suggested as being electrochemically inert.⁷⁻⁹ On the other hand, studies of isolated^{10,11,12} and randomly arranged two-dimensional networks of single walled carbon nanotubes (SWNTs)¹³ have shown that the sidewalls of SWNTs promote facile electron transfer. This provides an impetus to determine whether similar activity is evident in SWNT forests.

In this communication we investigate SWNT forest electrodes using a new nanoscale electrochemical cell technique,^{14, 15} which allows us to examine electrochemistry at characteristic sites - closed ends and sidewalls, in isolation. In essence, a nanopipet containing electrolyte solution and one or more reference / counter electrode(s) is used to make an electrochemical cell with a targeted region of a sample, which is connected as a working electrode. For the present application, this is particularly powerful, as any type of post processing, lithography¹⁰ or mechanical cutting of the SWNTs is avoided,¹⁶ allowing the study of the true electrochemical activity of the forests in the native, pristine, unprocessed state. For the studies described herein, SWNT forests, were grown using chemical vapour deposition (CVD). CVD was chosen for forest growth, in preference to chemical processing and vertical alignment via chemical binding to a substrate, as CVD enables high density, pristine, closed-end SWNTs to be grown directly. Chemical processing, results in cutting and shortening of the SWNTs and

incomplete coverage of the underlying conducting substrate.^{8, 17}

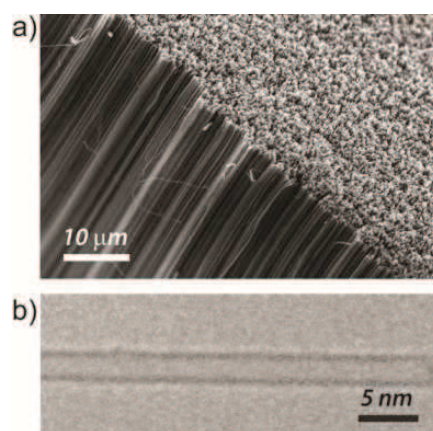


Figure 1. a) FE-SEM image of a SWNT forest. b) Typical TEM image of a SWNT extracted from a forest.

Figure 1 shows a representative field emission-scanning electron microscopy (FE-SEM) image of an a CVD as-grown SWNT forest (a) and a typical TEM image (b) of a SWNT extracted from the forest (CVD growth and characterisation details can be found in section 1, Supporting Information). The absence of any amorphous carbon is noteworthy. The high quality of the forests was further proven using micro-Raman spectroscopy on intact forests, recorded from both the SWNT ends and the sidewalls, as described in section 2, Supporting Information.

It was also particularly important to confirm that the ends of the forests were free from catalytic metal nanoparticles (NPs), since these can impact significantly on the electrochemical response of SWNTs.¹⁸⁻²¹ The results of X-ray photoelectron spectroscopy (XPS) are shown in Figure 2a, for the top surface of the forest (black line), and the surface of the cobalt (Co) catalyst (red line) after subjecting it to 'growth' conditions but without a carbon source (*i.e.* no actual growth). The catalyst sample shows a distinct cobalt 2p peak at 780 eV. Peaks at 75 eV and 530 eV are for aluminium (Al 2p) and oxygen (O 1s), respectively, from the aluminium oxide under-layer. In contrast, for the forest, the Co peak disappears and the spectrum is dominated by a carbon 1s peak at 290 eV.

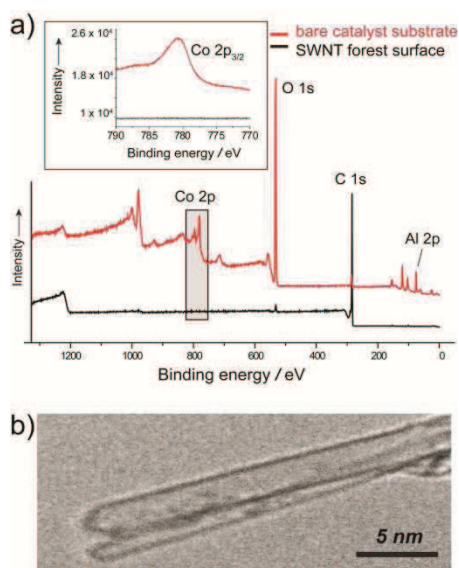


Figure 2. a) XPS spectra of bare catalyst substrate (red line) and SWNT forest surface (black line). The inset shows the spectral range corresponding to Co 2p_{3/2} for both SWNT forest (black line) and catalyst (red line) surfaces. b) Typical TEM image of SWNT ends.

Since the penetration depth of XPS is ca. 10 nm and the forest was ~500 μm thick, this analysis proves that these SWNT forests exhibit a root growth process,²² where the catalytic NPs reside at the base of the SWNT, *i.e.* on the substrate. There is a very small oxygen 1s peak, relative to C 1s, originating from the top 10 nm of the SWNT forest. This most likely results from a small degree of oxygenation of the SWNT forest under ambient conditions, but is insignificant compared to the signals obtained when a SWNT end is deliberately opened.^{8, 16} Further TEM images of SWNT ends, *e.g.* Figure 2b, confirmed that they were closed and free from catalyst NPs, the latter in agreement with the XPS data.

Figure 3a shows a photograph and schematic, respectively, of the experimental arrangement for the voltammetric measurements. More detailed information on the experimental arrangement is given in section 3, Supporting Information. The theta glass (double baralled) pipet tips, of typical inner diameter ~400 nm (accurately characterised using FE-SEM) were filled with the solution of interest, and Ag/AgCl quasi-reference counter electrodes (QRCEs) were placed in each barrel. With a bias applied between the two barrels the conductance current, which flows between barrels, via the meniscus at the end of the pipet tip, could be monitored. This enabled us to: (i) accurately position the tip, keeping the tip and meniscus in a fixed position during voltammetric measurements;^{14, 15} and (ii) assess the contact area of the meniscus with the area of interest on the SWNT forest. Figure 3b shows typical conductance current – voltage curves, recorded by sweeping the potential of one QRCE with respect to the other (held at ground), with 50 mM potassium chloride solution in the pipet. The pipet was maintained in a fixed position on the SWNT forest over the closed ends (blue line) and sidewalls (red line). A similar response is seen in both locations, which is close to that recorded for similar sized theta pipet tips on

hydrophobic impermeable substrates.²³ We thus conclude that the SWNT forest is not permeated to any significant extent by electrolyte from the pipet tip.

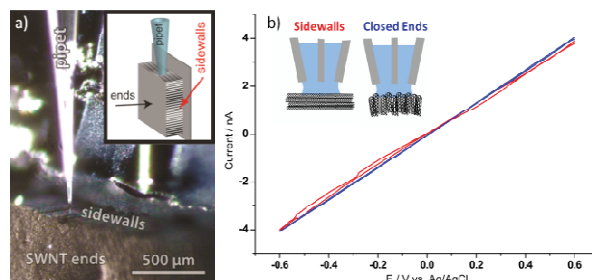


Figure 3. a) Digital photograph and schematic of the pipet in contact with the forest sidewalls, for voltammetric and conductance analysis. b) Current-voltage curves (forward and reverse) recorded on the closed tips (blue) and sidewalls (red), with a pipet of inner diameter 400 nm, containing 50 mM KCl, at 100 mV s⁻¹.

For redox measurements, the pipet was filled with solution containing both supporting electrolyte and the redox species of interest. Once contact had been made between the pipet meniscus and forest, cyclic voltammetric (CV) measurements were carried out at different spots on several samples, at both the forest ends and the sidewalls, with the SWNT forest connected as the working electrode. Two well-known outer sphere, redox couples, with very different formal potentials (E^0 values), (ferrocenylmethyl) trimethylammonium, (FcTMA⁺²⁺)¹⁰ and hexaammineruthenium (Ru(NH₃)₆^{3+/2+}), were used to probe the local electrochemical response. Figure 4 and section 3, Supporting Information, show typical CVs recorded at the SWNT ends and sidewalls. These data clearly show that, for both couples, the electrochemical response is comparable with a difference in the 1/4-wave and 3/4-wave potential, $E_{1/4} - E_{3/4}$, in the range 57 – 64 mV, indicating that the reactions are close to reversible in all locations.

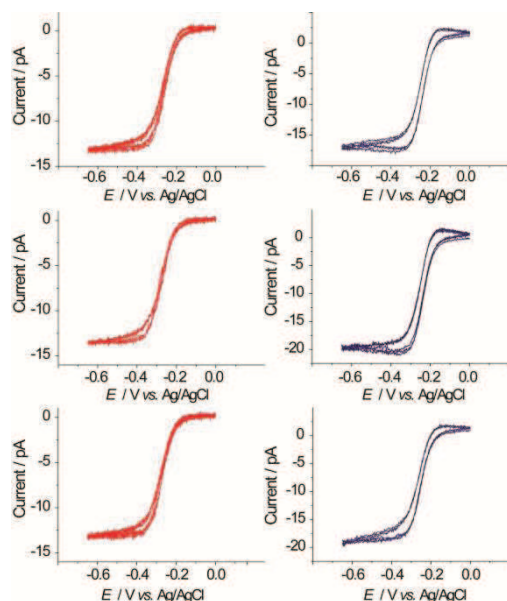


Figure 4. Typical CVs of 5 mM Ru(NH₃)₆³⁺ reduction in 50 mM KCl at a scan rate of 100 mV s⁻¹. Red lines indicate forest sidewalls, blue lines, forest closed ends.

The mass transfer rate coefficient (k_t) for this pipet electrode arrangement is estimated as $\sim 0.03 \text{ cm s}^{-1}$, from simple analysis of the limiting current. Hence, the effective standard heterogeneous electron transfer rate constant in both areas is much larger. Since k_t is higher than that experienced in standard CV experiments (at scan rates up to ca. 5 V s^{-1}), we deduce that SWNT forests should display essentially reversible behaviour for most common electrochemical techniques for outer sphere redox couples. Thus, both the closed ends and sidewalls of CVD grown SWNT forests should be considered highly electrochemically active, and capable of fast electron transfer. Furthermore, it should not be necessary, as has been suggested by others,^{9, 24-28} to carry out any pretreatment or activation of CVD-grown SWNTs for electrochemical studies and measurements with redox couples of this type. Note that for some inner sphere processes which may need to bind directly with the electrode surface in order to undergo efficient electron transfer,²⁹ the chemical nature of the surface (and whether the end is open or closed) may be more important.

In summary, we have demonstrated a novel approach for interrogating the electrochemistry of different parts of SWNTs in a forest arrangement, using a mobile nanoscopic electrochemical cell. In this way the electrochemical activity of the forest, or for that matter, any complex sample, can be studied in its native state, in any desired location, at high spatial resolution, without the need for sample processing. Using this arrangement, we have proved that a SWNT end does not need to be open for it support fast electrochemistry with outer sphere redox couples. This overturns the present consensus that the electrochemistry of SWNTs is dominated by open ends^{8, 9, 30, 31} formulated from the results of CV measurements averaged over macro-sized areas of SWNTs assembled on conducting surfaces.

The studies herein provide further convincing direct evidence for the considerable activity of SWNT sidewalls,^{10, 11,12} in contrast to various indirect studies which have suggested that such sites are electrochemically inert.^{9, 24, 25} More generally, direct nanoscopic studies – such as those reported herein – are providing a new consensus that the basal surface of various related sp^2 carbon materials promotes fast electron transfer.^{15,32,33}

Notes and references

^aDept. of Chemistry, Uni of Warwick, Coventry, CV4 7AL, UK.
Fax: (+44) 02476 524112; E-mail: j.macpherson@warwick.ac.uk;
p.r.unwin@warwick.ac.uk

[†] TSM and NE contributed equally to the work

The authors thank Dr. David Burt, Mr. Jonathan Newland and Dr. Petr V. Dudin for their contributions to the work. We thank the EPSRC for access to the XPS at NCESS (UK). Equipment used in this research was obtained through Science City (AM2), with support from Advantage West Midlands and part funded by the European regional Development Fund. This project was supported by the European Research Council through project ERC-2009-AdG 247143-QUANTIF, a Marie Curie IntraEuropean Fellowship (236885) and EPSRC (EP/H023909/1), with additional funding from the UK National Physical Laboratory.

[†] Electronic Supplementary Information (ESI) available: 1. SWNT forest growth and characterisation. 2. MicroRaman Microscopy of SWNT forests. 3. Voltammetric Measurements. See DOI: 10.1039/b000000x/

1. D. N. Futaba, K. Hata, T. Yamada, T. Hiraoka, Y. Hayamizu, Y. Kakudate, O. Tanaike, H. Hatori, M. Yumura and S. Iijima, *Nat. Mater.*, 2006, **5**, 987-994.
2. S. Fan, M. G. Chapline, N. R. Franklin, T. W. Tombler, A. M. Cassell and H. Dai, *Science*, 1999, **283**, 512-514.
3. H. Huang, C. H. Liu, Y. Wu and S. Fan, *Advanced Materials*, 2005, **17**, 1652-1656.
4. J. Wang, *Electroanalysis*, 2005, **17**, 7-14.
5. X. Yu, B. Munge, V. Patel, G. Jensen, A. Bhirde, J. D. Gong, S. N. Kim, J. Gillespie, J. S. Gutkind, F. Papadimitrakopoulos and J. F. Rusling, *J. Am. Chem. Soc.*, 2006, **128**, 11199-11205.
6. D. J. Garrett, P. A. Brooksby, F. J. Rawson, K. H. R. Baronian and A. J. Downard, *Anal. Chem.*, 2011, **83**, 8347-8351.
7. J. Li, A. Cassell, L. Delzeit, J. Han and M. Meyyappan, *J. Phys. Chem. B*, 2002, **106**, 9299-9305.
8. A. Chou, T. Bocking, N. K. Singh and J. J. Gooding, *Chem. Commun.*, 2005, 842-844.
9. A. F. Holloway, K. Toghill, G. G. Wildgoose, R. G. Compton, M. A. H. Ward, G. Tobias, S. A. Llewellyn, B. Ballesteros, M. L. H. Green and A. Crossley, *J. Phys. Chem. C*, 2008, **112**, 10389-10397.
10. I. Heller, J. Kong, H. A. Heering, K. A. Williams, S. G. Lemay and C. Dekker, *Nano Lett.*, 2005, **5**, 137-142.
11. J. Kim, H. Xiong, M. Hofmann, J. Kong and S. Amemiya, *Anal. Chem.*, 2010, **82**, 1605-1607.
12. P. V. Dudin, M. E. Snowden, J. V. Macpherson and P. R. Unwin, *ACS Nano*, 2011, **5**, 10017-10025.
13. I. Dumitrescu, P. V. Dudin, J. P. Edgeworth, J. V. Macpherson and P. R. Unwin, *J. Phys. Chem. C*, 2010, **114**, 2633-2639.
14. N. Ebejer, M. Schnipper, A. W. Colburn, M. A. Edwards and P. R. Unwin, *Anal. Chem.*, 2010, **82**, 9141-9145.
15. S. C. S. Lai, A. N. Patel, K. McKelvey and P. R. Unwin, *Angew. Chemie Intl. Ed.*, 2012, in press. DOI: 10.1002/anie.201200564
16. K. Gong, S. Chakrabarti and L. Dai, *Angew. Chemie Intl. Ed.*, 2008, **47**, 5446-5450.
17. X.-J. Huang, H.-S. Im, O. Yarimaga, J.-H. Kim, D.-Y. Jang, D.-H. Lee, H.-S. Kim and Y.-K. Choi, *J Electroanal. Chem.*, 2006, **594**, 27-34.
18. M. Pumera, *Langmuir*, 2007, **23**, 6453-6458.
19. J. Kruusma, N. Mould, K. Jurkschat, A. Crossley and C. E. Banks, *Electrochem. Commun.*, 2007, **9**, 2330-2333.
20. M. Pumera and H. Iwai, *J. Phys. Chem. C*, 2009, **113**, 4401-4405.
21. E. J. E. Stuart and M. Pumera, *J. Phys. Chem. C*, 2010, **114**, 21296-21298.
22. K. Hata, D. N. Futaba, K. Mizuno, T. Namai, M. Yumura and S. Iijima, *Science*, 2004, **306**, 1362-1364.
23. M. E. Snowden, A. G. Güell, S. C. S. Lai, K. McKelvey, N. Ebejer, M. A. O'Connell, A. W. Colburn and P. R. Unwin, *Anal. Chem.*, 2012, **84**, 2483-2491.
24. R. L. McCreery, *Chem. Rev.*, 2008, **108**, 2646-2687.
25. M. Pumera, *Chem.-Eur. J.*, 2009, **15**, 4970-4978.
26. C. E. Banks and R. G. Compton, *Analyst*, 2006, **131**, 15-21.
27. C. E. Banks, T. J. Davies, G. G. Wildgoose and R. G. Compton, *Chem. Commun.*, 2005, 829-841.
28. C. E. Banks, R. R. Moore, T. J. Davies and R. G. Compton, *Chem. Commun.*, 2004, 1804-1805.
29. A. J. Bard, *J. Am. Chem. Soc.*, 2010, **132**, 7559-7567.
30. J. J. Gooding, R. Wibowo, J. Liu, W. Yang, D. Losic, S. Orbons, F. J. Mearns, J. G. Shapter and D. B. Hibbert, *J. Am. Chem. Soc.*, 2003, **125**, 9006-9007.
31. J. Liu, A. Chou, W. Rahmat, M. N. Paddon-Row and J. J. Gooding, *Electroanalysis*, 2005, **17**, 38-46.
32. I. Dumitrescu, P. R. Unwin and J. V. Macpherson, *Chem. Commun.*, 2009, 6886-6901.
33. A. G. Güell, N. Ebejer, M. E. Snowden, J. V. Macpherson and P. R. Unwin, *J. Am. Chem. Soc.* in press DOI 10.1021/ja3014902

Supporting Information

Electrochemistry at Carbon Nanotube Forests: Sidewalls and Closed Ends Allow Fast Electron Transfer

Thomas S. Miller, Neil Ebejer, Aleix G. Güell, Julie V. Macpherson and Patrick R. Unwin

Section 1: SWNT forest growth and characterisation

SWNT forests were grown on silicon wafers (n-type, 525 μm thick, IDB Technologies Ltd, UK) which had been sputtered (Plassys (MP 900S)) with a 10 nm layer of aluminium (Al) and cleaved into $\sim 1\text{ cm} \times 1.5\text{ cm}$ pieces. The individual substrates were ashed in an oxygen plasma for 2 minutes (K1050X plasma system, Emitech, UK; O_2 pressure 6×10^{-1} mbar) and sputtered (Quorum Technologies SC7640 sputter coater, fitted with a Co target, 99.95%, Testbourne Ltd. UK) with Co. Once prepared, the substrates were heated to growth temperature (T_G) in a CVD oven consisting of a 1" diameter quartz tube (Enterprise Q Ltd.) passing through a tube furnace (Lindberg/Blue M, Thermo-Fisher Scientific, US). Heating was performed under hydrogen flow (99.995%, BOC). After T_G was reached, argon (99.9995%, BOC) was bubbled through ethanol (99.99%, Fisher Scientific) at 0 $^\circ\text{C}$ before being introduced into the CVD system as the source of carbon. In both cases, the flow rates of the process gasses were controlled using mass flow controllers (MKS Instruments UK Ltd, UK). Growth was sustained for 40 minutes before the Ar-EtOH flow was stopped and the oven was allowed to cool under hydrogen flow.

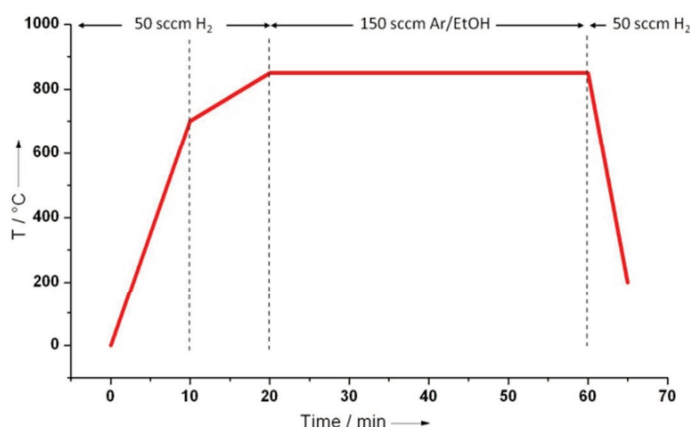


Fig S1. Graphic representation of the growth scheme

FE-SEM images were acquired using a Zeiss SUPRA 55 VP FE-SEM using a 1 kV accelerating voltage. TEM images were taken using a Jeol 2000FX TEM. SWNTs were deposited onto lacey carbon film coated TEM grids (Agar Scientific) by rubbing the grid onto the side of the forest. This was found to introduce less contamination than solution based methods. XPS spectra were taken using a Scienta ESCA300 photoelectron spectrometer, with a monochromated rotating anode Al $K\alpha$ X-ray source at the National Centre for Electron Spectroscopy and Surface analysis, Daresbury Laboratory, UK.

Section 2: Micro-Raman Microscopy of SWNT forests

Micro-Raman spectra were collected using a Renishaw inVia Raman microscope fitted with a CCD detector and a 633 nm HeNe laser with a spot size of 3 μm with a 5 % attenuation. By

Supporting Information

tilting the sample we were able to focus onto the sidewalls, allowing us to obtain Raman spectra of this face. The shape and location of the G band (sp^2) at 1589 cm^{-1} , in both spectra in Figure S2, is indicative of SWNTs.^{1,2} Whilst small D peaks (sp^3 carbon) are visible, G / D ratios for the ends and the sidewalls, 7:1 and 9:1 respectively, indicate significantly higher quality forests (*i.e.* cleaner, lower defect density) than those previously described in the literature.^{2,3}

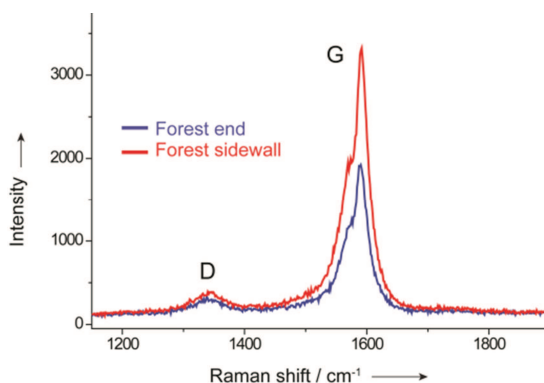


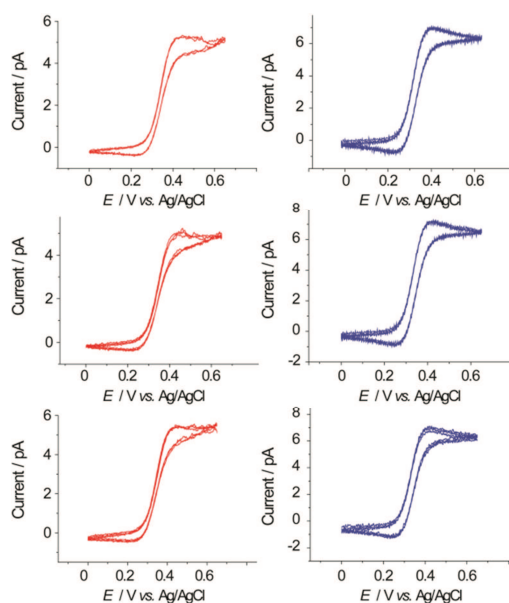
Fig S2. Micro-Raman spectra of an intact SWNT forest focusing on the sidewalls and tube ends.

Section 3: Voltammetric Measurements

To produce an electrical contact to the SWNT forest, a 200 nm thick gold film was evaporated onto half of the sample, covering both the tops and sides, by means of a shadow mask, leaving the rest of the sample intact for electrochemical analysis. The sample was then mounted to align either the top of the forest or the sidewalls, for electrochemical interrogation. The pipet tips were produced by pulling theta glass borosilicate pipets (Harvard Apparatus) using a Sutter instruments P2000 laser puller. Pipets were filled with the solution of interest and Ag/AgCl quasi-reference electrodes were placed in each barrel. Pipets of inner diameter $\sim 400\text{ nm}$ were routinely employed herein and were accurately characterised using FE-SEM. The pipet was translated towards the surface using a piezoelectric actuator (Physik Instrumente (PI) Nanocube), in conjunction with in-house written software (LABVIEW). During approach, a potential bias, corresponding to the diffusion-limited oxidation/reduction potential of the mediator of interest was applied to one barrel of the capillary, whilst the SWNT forest substrate was held at ground. A current was sensed as soon as the meniscus at the end of the capillary established contact with the SWNT forest substrate; at this point the approach was automatically stopped. All electrochemical experiments were performed at room temperature, 293 K, and potentials quoted against Ag/AgCl (50mM KCl).

Figure S3 shows typical CVs recorded on the sidewall and closed ends of the SWNT forest for oxidation of the redox mediator FcTMA^+ .

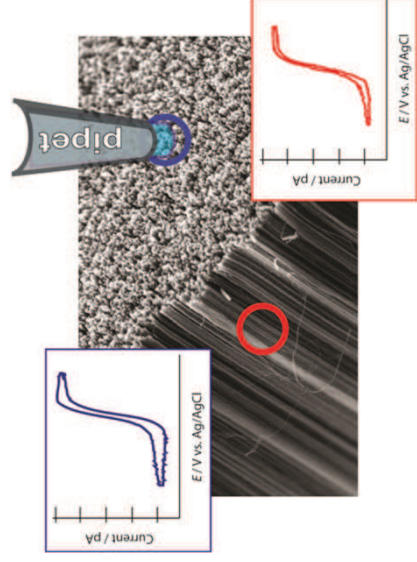
Supporting Information



FigS3. CVs of 2 mM FcTMA^{+/2+} oxidation in 50 mM KCl at a scan rate of 100 mV s⁻¹. Red lines indicate forest sidewalls, blue lines, the forest closed ends.

References

1. M. S. Dresselhaus, G. Dresselhaus, R. Saito and A. Jorio, *Phys. Reports*, 2005, **409**, 47-99.
2. D. P. Burt, W. M. Whyte, J. M. R. Weaver, A. Glidle, J. P. Edgeworth, J. V. Macpherson and P. S. Dobson, *J. Phys. Chem. C*, 2009, **113**, 15133-15139.
3. K. Gong, S. Chakrabarti and L. Dai, *Angew. Chemie Intl. Ed.*, 2008, **47**, 5446-5450.



Using a nanoscale electrochemical cell both the sidewalls and closed ends of a SWNT forest are shown to support fast electron transfer